Single Image Reflection Removal with Absorption Effect (Supplementary Material)

Qian Zheng[1]* Boxin Shi[2,3,4]* Jinnan Chen[1] Xudong Jiang[1] Ling-Yu Duan[2,4] Alex C. Kot[1]

[1]School of Electrical and Electronic Engineering, Nanyang Technological University, Singapore
[2]NELVT, Department of Computer Science and Technology, Peking University, Beijing, China
[3]Institute for Artificial Intelligence, Peking University, Beijing, China
[4]Peng Cheng Laboratory, Shenzhen, China
{zhengqian, exdjiang, eackot}@ntu.edu.sg, {shiboxin, lingyu}@pku.edu.cn, jinnan001@e.ntu.edu.sg

This file provides (i) experiments of fitting e on real data (footnote 2) (ii) results on a testing data with glass color variation (footnote 5), (iii) more visual quality comparison results (footnote 11), and (iv) comparison results with the single-step method (footnote 12).

7. Fitting e Using Data from SIR^2 [8]

We take data in SIR^2 to examine our image formation model that considers the absorption effect. We fit e based on a small patch $\mathbf{I}_p$ instead of the whole image $\mathbf{I}$ to reduce the impact of reflection (Figure 7 left). To be specific, if the patch is with $(\mathbf{\Phi R})_p \approx 0$ ($\mathbf{\Phi}$ is provided by SIR^2), e can be approximated by $\text{avg}(\mathbf{I}_p \oslash \mathbf{T}_p)$ according to Equation (5), as $\mathbf{O}$ tends to be an all-one matrix. It is noted that the absolute value of e fitted by LDR images in SIR^2 is not accurate due to the non-linear camera pipeline. To this end, our analysis is based on the relative values of e fitted from a pair of $\mathbf{I}$ that has a similar transmission (SSIM>0.95) but different glass thickness. We then locate the patch for a pair of images such that $(\mathbf{\Phi R})_p \approx 0$ (more than 500 elements for a 50×50 patch in both samples) to estimate e. Finally, we find 30 eligible pairs from SIR^2 for analysis (Figure 7 right top). We also randomly synthesize 300 pairs of data with different glass thickness (Figure 7 right bottom) for reference which are less affected by camera pipeline. Figure 7 shows that most $\mathbf{I}$ with the thin glass (less absorption) has larger e, which is consistent with our modeling of absorption effect.

8. Testing on Data with Different Glass Colors

We have validated the effectiveness of our methods to consider the absorption effect in aspects of glass thickness and orientation on real data (Table 1 in the main paper). In this section, we further investigate the performance on data with various absorption effects caused by the color of glass.

Data synthesizing. Since there is no existing real dataset with the color variation of glass, we use a synthetic dataset BLD-COLOR for evaluation. BLD-COLOR is rendered based on a physically-based rendering engine Cycles [10]

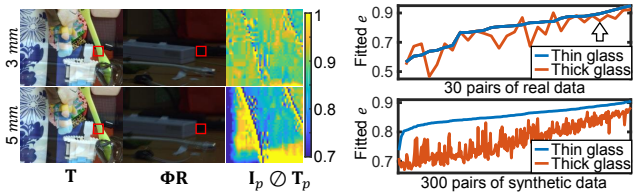

Figure 7. Left: $\mathbf{T}$ and $\mathbf{\Phi R}$ of a pair of data (thickness: 3 mm and 5 mm); Red boxes indicate patch location; Heat maps visualize fitted e on the patch (for each pixel). Right top: Fitted e for 30 pairs of real data from SIR^2; The arrow indicates data in left figure. Right bottom: Fitted e for 300 pairs of synthetic data (by Equation (5)).

and a free open-source 3D computer graphics software Blender[a]. We synthesize 90 reflection-contaminated images using three demo scenarios (two indoor, one outdoor)[b]. Specifically, a glass is inserted into these scenarios and 15 scenes are rendered by placing the glass and camera at different positions (5 for each of these three scenarios). These positions are randomly selected. For each scene, we change the color of the glass by setting its V channel (with HSV color model, denoted as V_c) to 1.0, 0.98, 0.96, 0.94, 0.92, 0.90 and generate 6 reflection-contaminated images accordingly. Figure 8 shows the rendered reflection-contaminated images as well as their transmission images of three scenes from three scenarios. We use the same evaluation strategy as that in our main paper to compare performance on this synthetic dataset.

Overall performance. Table 3 displays quantitative results. As can be observed, our method and our one-branch method achieve the best and the second-best results in terms of SSIM, IS, and PSNR. Such results validate the effectiveness of our method that considers absorption effect to solve the problem of single image reflection removal.

*Corresponding authors.

[a]https://www.blender.org/

[b]Tagged by AGENT 327 BARBERSHOP, CLASS ROOM, and BARCELONA PAVILLION. Available from https://www.blender.org/download/demo-files/#cycles

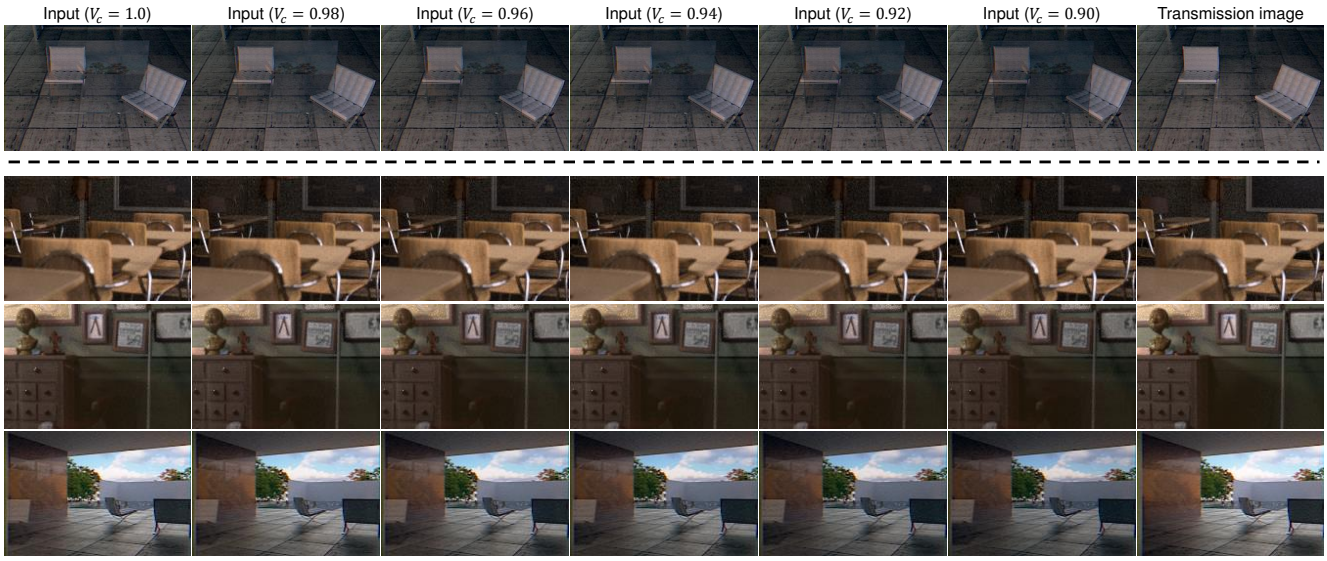

Figure 8. An illustration of BLD-COLOR dataset. From top to bottom: a synthetic scene indicating the color of glass for each column, three scenes from AGENT 327 BARBERSHOP, CLASS ROOM, and BARCELONA PAVILLION, respectively. From left to right: reflection-contaminated images with different colors of glass ($V_c = 1.0, 0.98, 0.96, 0.94, 0.92, 0.90$, respectively) and a transmission image.

Table 3. Comparisons of quantitative results in terms of SSIM, IS, and PSNR on BLD-COLOR. We mark the best and second-best performing methods in red and blue respectively.

Dataset(size)	Metric	Ours	One-branch	*w/o*-Con	ZN18[1]	YM19[2]	WS19[3]	WT19[4]	WY19[5]	KH20[6]	LY20[7]
BLD-COLOR	SSIM	**0.8067**	**0.8004**	0.7991	0.7934	0.7825	0.7369	0.7739	0.7483	0.7646	0.7772
	IS	**0.9253**	**0.9222**	0.9189	0.9160	0.9118	0.8511	0.9196	0.9191	0.9159	0.9169
	PSNR	**23.63**	**23.60**	23.27	22.24	23.52	19.28	22.66	22.38	22.89	22.19

Table 4. Comparisons of quantitative results in terms of SSIM, IS, and PSNR for our method and one-step method. We bold the better numbers.

Datasets	SSIM		IS		PSNR	
	Two-step	One-step	Two-step	One-step	Two-step	One-step
SIR^2-THICK [8]	**0.8965**	0.8741	**0.9773**	0.9612	**24.05**	22.89
ZC20-ORIEN [9]	**0.8790**	0.8511	**0.9722**	0.9521	**23.93**	19.24
LY20-DATA [7]	**0.8732**	0.8611	**0.9552**	0.9477	**23.97**	22.44
SIR^2 [8]	**0.9003**	0.8843	**0.9756**	0.9671	**24.34**	23.01
ZN18-DATA [1]	**0.7783**	0.7615	**0.8970**	0.8910	**19.63**	18.87
BLD-COLOR	**0.8067**	0.7977	**0.9222**	0.9169	**23.63**	23.38

9. Visual Quality Comparison Results

Figure 9-Figure 14 show more visual quality results, comparing with methods of one-branch, *w/o*-Con, YM19 [2], ZN18 [1], WS19 [3], WT19 [4], WY19 [5], KH20 [6], and LY20 [7], on datasets of SIR^2-THICK [8], ZC20-ORIEN [9], LY20-DATA [7], SIR^2 [8], ZN18-DATA [1], and BLD-COLOR. For each result (or input), we calculate the IS index map between it and the ground truth of transmission image and put the IS index map at bottom of each image. All heat maps take the same number-color correspondence as that in Figure 5 in the main paper. The better results of reflection removal and the IS index maps demonstrate that our method not only recovers more accurate overall intensity of transmission images but also better suppresses reflection artifacts for reflection removal.

10. Comparing with One-Step Method

To validate the effectiveness of our two-step method, we compare it with a one-step method. This one-step method is developed with only network h and takes $\mathbf{I}$ as the input, as compared with our two-step method in Figure 2 in our main paper. We use the same training data and the same training setting as those for our two-step method to train the one-step method.

The quantitative performance comparison is displayed in Table 4. As can be observed, our two-step method shows a significant performance advantage over the one-step method. The superior performance of our method for testing datasets validates the effectiveness of our two-step method that considers the absorption effect in the first step.

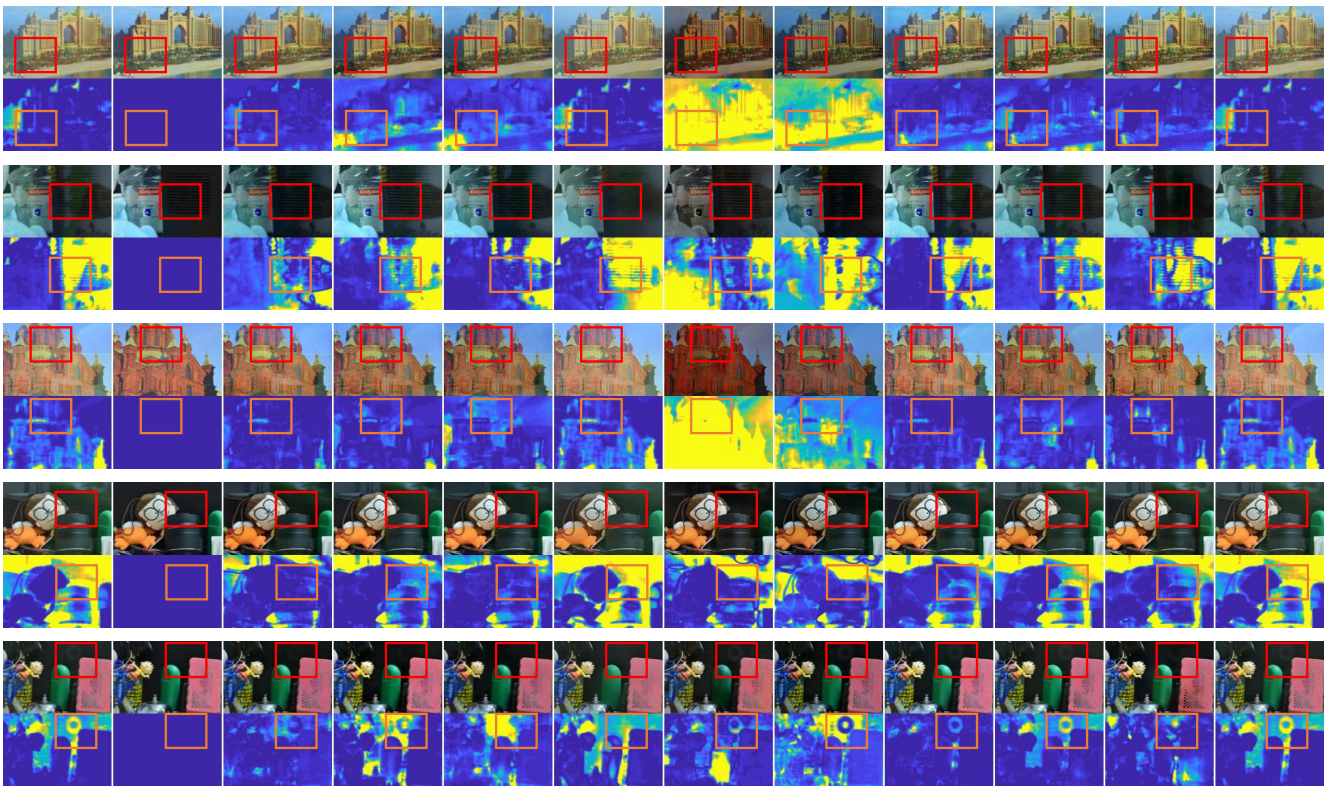

Figure 9. Visual quality comparison for data from SIR^2-THICK [8]. Color boxes highlight noticeable differences. Zoom in for better details.

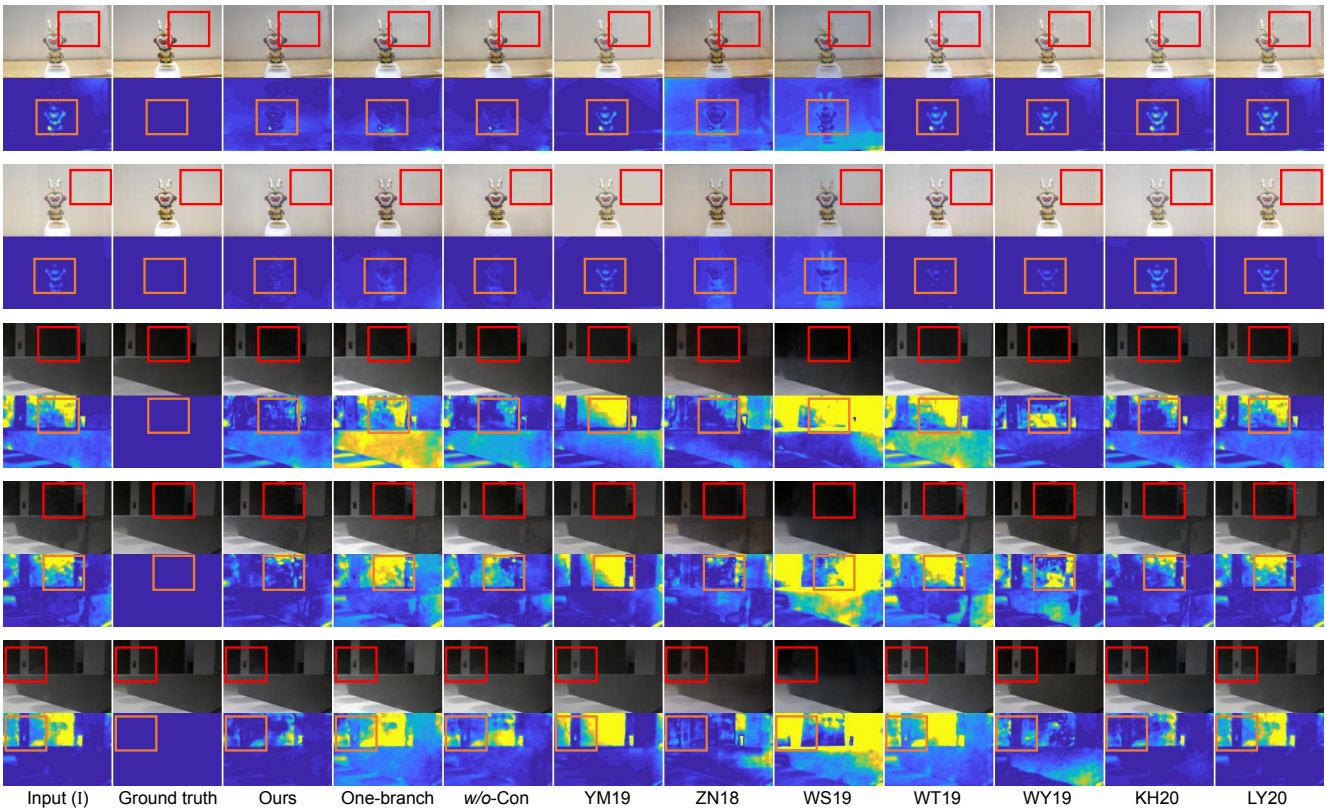

Figure 10. Visual quality comparison for data from ZC20-ORIEN [9]. Color boxes highlight noticeable differences. Zoom in for better details.

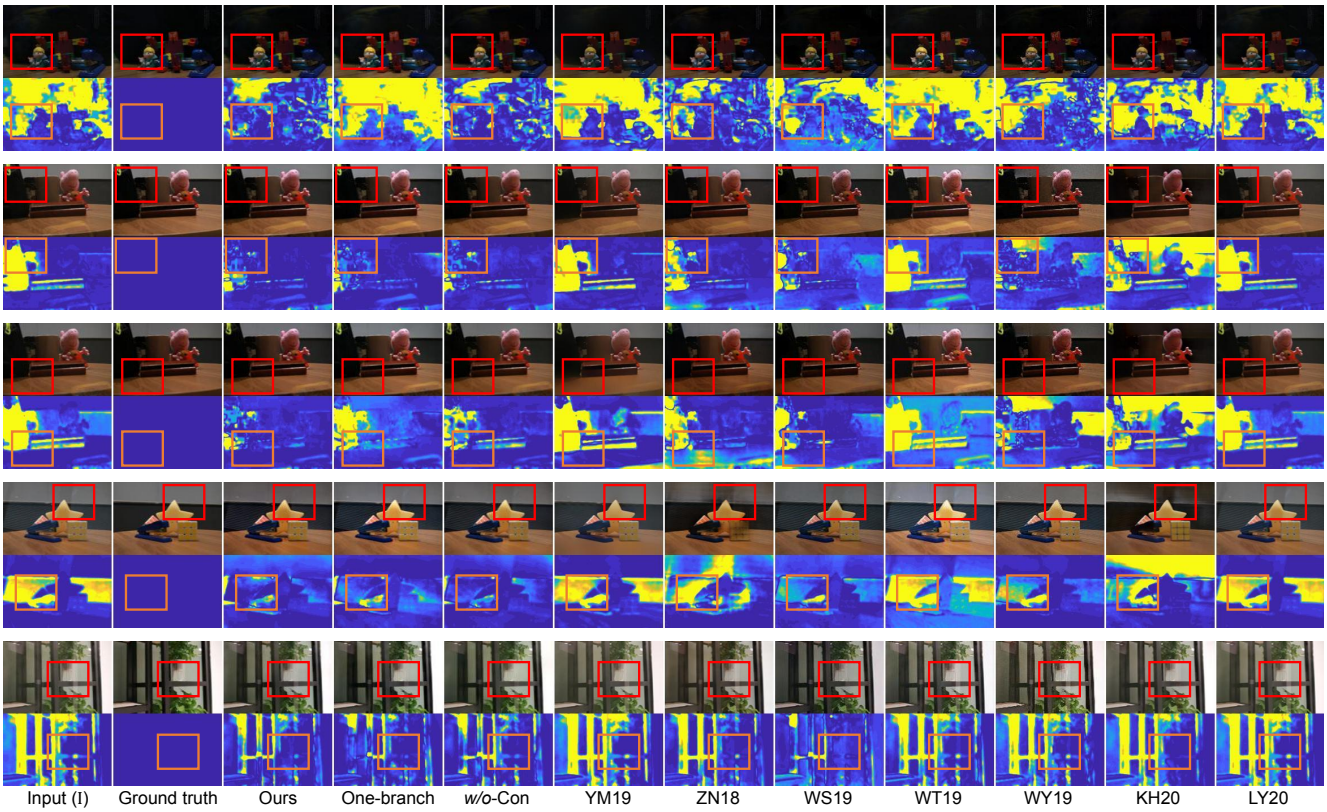

Figure 11. Visual quality comparison for data from LY20-DATA [7]. Color boxes highlight noticeable differences. Zoom in for better details.

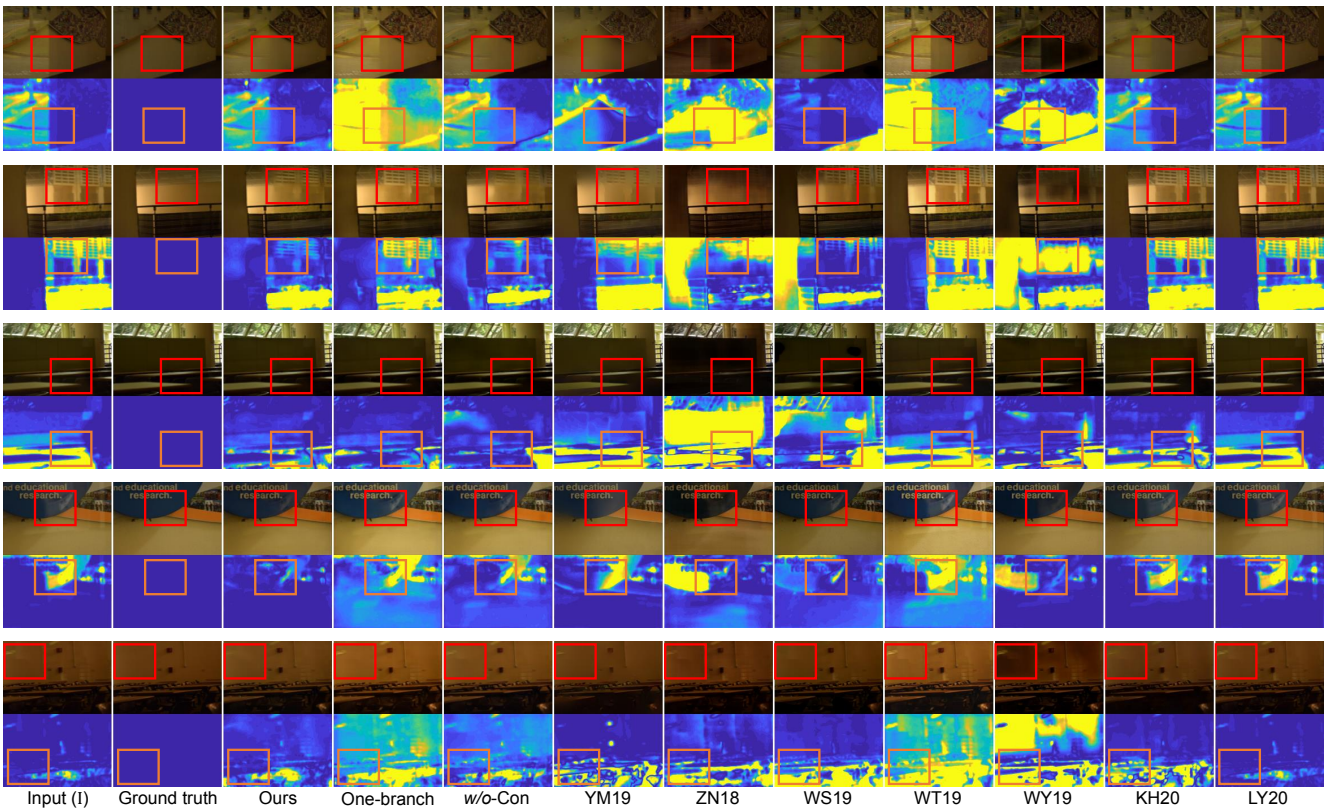

Figure 12. Visual quality comparison for data from SIR^2 [8]. Color boxes highlight noticeable differences. Zoom in for better details.

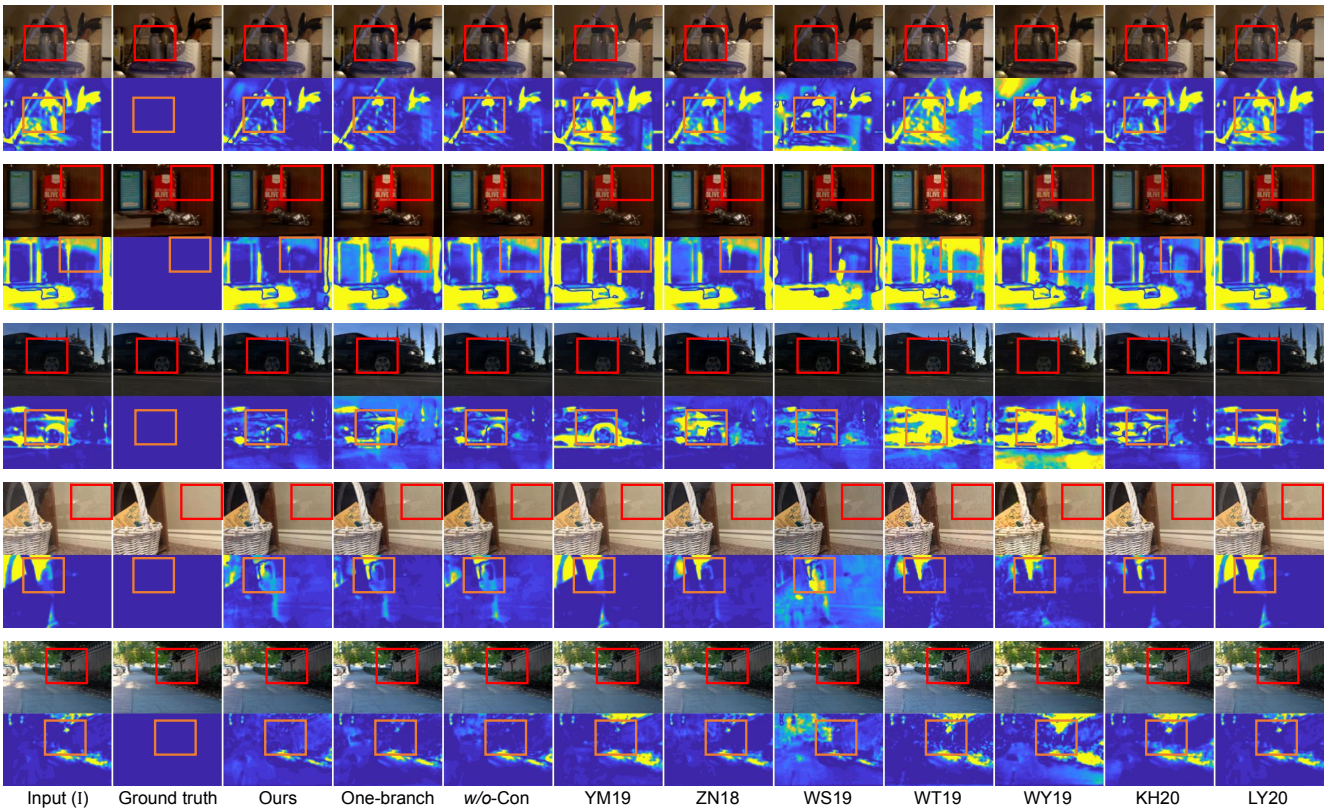

Figure 13. Visual quality comparison for data from ZN18-DATA [1]. Color boxes highlight noticeable differences. Zoom in for better details.

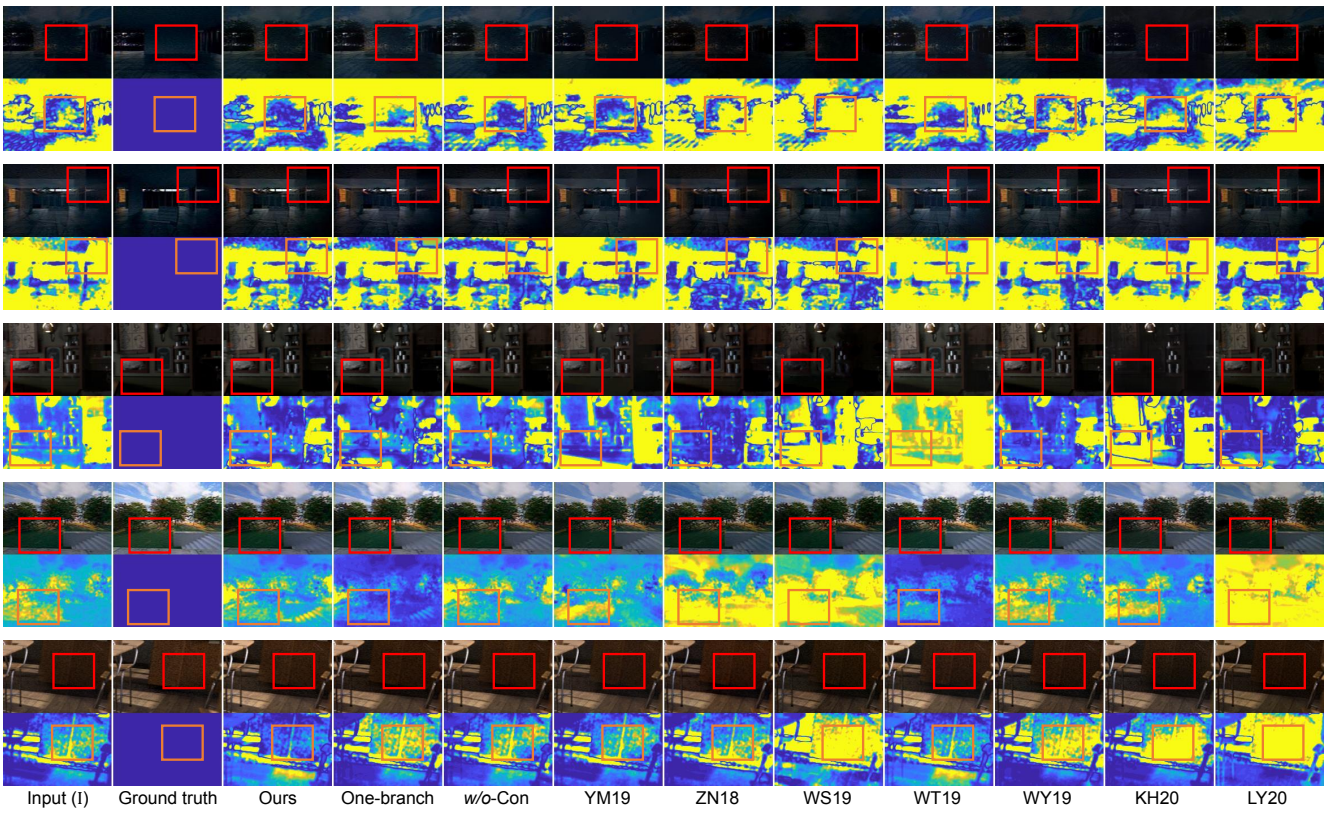

Figure 14. Visual quality comparison for data from BLD-COLOR. Color boxes highlight noticeable differences. Zoom in for better details.

References

[1] X. Zhang, R. Ng, and Q. Chen, "Single image reflection separation with perceptual losses," in *Proc. of Computer Vision and Pattern Recognition*, 2018. 2, 5

[2] Y. Yang, W. Ma, Y. Zheng, J.-F. Cai, and W. Xu, "Fast single image reflection suppression via convex optimization," in *Proc. of Computer Vision and Pattern Recognition*, 2019. 2

[3] R. Wan, B. Shi, H. Li, L.-Y. Duan, A.-H. Tan, and A. K. Chichung, "CoRRN: Cooperative reflection removal network," *IEEE Transactions on Pattern Analysis and Machine Intelligence*, 2019. 2

[4] Q. Wen, Y. Tan, J. Qin, W. Liu, G. Han, and S. He, "Single image reflection removal beyond linearity," in *Proc. of Computer Vision and Pattern Recognition*, 2019. 2

[5] K. Wei, J. Yang, Y. Fu, D. Wipf, and H. Huang, "Single image reflection removal exploiting misaligned training data and network enhancements," in *Proc. of Computer Vision and Pattern Recognition*, 2019. 2

[6] S. Kim, Y. Huo, and S.-E. Yoon, "Single image reflection removal with physically-based training images," in *Proc. of Computer Vision and Pattern Recognition*, June 2020. 2

[7] C. Li, Y. Yang, K. He, S. Lin, and J. E. Hopcroft, "Single image reflection removal through cascaded refinement," in *Proc. of Computer Vision and Pattern Recognition*, June 2020. 2, 4

[8] R. Wan, B. Shi, L.-Y. Duan, A.-H. Tan, and A. C. Kot, "Benchmarking single-image reflection removal algorithms," in *Proc. of Internatoinal Conference on Computer Vision*, 2017. 1, 2, 3, 4

[9] Q. Zheng, J. Chen, Z. Lu, B. Shi, X. Jiang, K.-H. Yap, L.-Y. Duan, and A. C. Kot, "What does plate glass reveal about camera calibration," in *Proc. of Computer Vision and Pattern Recognition*, 2020. 2, 3

[10] Cycles, https://www.cycles-renderer.org/. 1